Available online at www.sciencedirect.com
SCIENCE DIRECT
Journal of Catalysis 236 (2005) 270–281
JOURNAL OF CATALYSIS
www.elsevier.com/locate/jcat

Bimetallic effects in the liquid-phase hydrogenation of 2-butanone

J.P. Breen [a,*], R. Burch [a], K. Griffin [b], C. Hardacre [a], M. Hayes [b], X. Huang [a], S.D. O'Brien [a]

[a] *CenTACat, Queen's University Belfast, David Keir Building, Stranmillis Road, Belfast BT9 5AG, N. Ireland, UK*
[b] *Johnson Matthey plc, Orchard Road, Royston, Hertfordshire, SG8 5HE, UK*

Received 6 July 2005; revised 27 September 2005; accepted 1 October 2005

Available online 7 November 2005

Abstract

A series of bimetallic Ru-containing monometallic and bimetallic catalysts were prepared and tested for their activity for the hydrogenation of 2-butanone to 2-butanol at 30 °C and 3 bar H_2. RuPt bimetallic catalysts were the most active for the reaction, with a ratio of 5 wt% Ru:1 wt% Pt on activated carbon (AC) found to be optimum. The activity of this bimetallic catalyst was more than double that of the sum of the activities of the monometallic Ru and Pt catalysts, providing evidence of a "bimetallic" effect. Structural analysis of the bimetallic catalysts revealed that they consisted of clusters of particles of the order of 1–2 nm. Extended X-ray absorption fine structure analysis showed that there were two types of particle on the surface of the bimetallic RuPt catalyst, specifically monometallic Ru and bimetallic RuPt particles. For the bimetallic particles, it was possible to fit the data with a model in which a Ru core of 1.1 nm is enclosed by two Pt-rich layers, the outer layer containing only 13 at% Ru. Pretreatment of the monometallic and bimetallic catalysts in hydrogen had a significant effect on the activity. Both the bimetallic and monometallic Ru-based catalysts showed a trend of decreasing activity with increasing temperature of prereduction in hydrogen. This loss of activity was almost fully reversible by exposure of the catalysts to air after reduction. The changing activity with exposure to different gas phase environments could not be attributed to changes in particle size or surface composition. It is proposed that the introduction of hydrogen results in a gradual smoothing of the surface and loss of defect sites; this process being reversible on introduction of air. These defect sites are particularly important for the dissociative adsorption of hydrogen, potentially the rate-determining step in this reaction.

Keywords: Bimetallic; Monometallic; Ruthenium; Platinum; EXAFS; TEM; EDX; XPS; Hydrogenation; 2-Butanone; MEK

1. Introduction

Bimetallic catalysts are at present the subject of considerable interest in heterogeneous catalysis, due to the fact that their catalytic properties can be superior to those of monometallic catalysts for many reactions [1]. The discovery of bimetallic catalysts has, in fact, been one of the major technical developments in heterogeneous catalysis [2] and it is now widely acknowledged that the addition of the second metal provides a method of controlling the activity, selectivity, and stability of the catalysts in certain reactions [3]. Various bimetallic combinations have been used successfully for different reactions. Pt–Re catalysts are used commercially as reforming catalysts. Binary Pt alloys, such as Pt–Ru or Pt–Sn, have been suggested as catalysts for the fabrication of fuel cell anodes with increased CO tolerance [4,5]. Bimetallic catalysts have been studied for various hydrogenation reactions [6–12]. Thomas and co-workers have done much research on the preparation and characterisation of ruthenium [13] and ruthenium-containing bimetallic catalysts [14–18]. They have pioneered a method of anchoring well-defined bimetallic ensembles within mesoporous silica pores to produce catalysts that are active and selective for various hydrogenation reactions. The activity was found to be dependent on the nature of the second metal added to ruthenium, the ratio of ruthenium to the second metal, and the cluster size. They found that Ru/Pt bimetallic catalysts were particularly active for the hydrogenation of cyclohexene [19].

It is not clear exactly what role the metal promoter plays in enhancing catalytic activity; it may have a direct role as an active centre for the reaction or may simply modify the active component. It is also not clear if the two metals form alloys,

* Corresponding author. Fax: +44 28 90382117.
E-mail address: j.breen@qub.ac.uk (J.P. Breen).

0021-9517/$ – see front matter
doi:10.1016/j.jcat.2005.10.004

if surface segregation of one element occurs, or if the two elements are randomly distributed on the surface of the catalyst [20]. Several authors have suggested a synergistic effect whereby catalytic performance is enhanced by the synergy between the component elements at the nanoscale [21–23]. The role of the second metal is sometimes simply to overcome a limiting side reaction or to promote a certain part of the reaction. In some cases the promoter metal shows no activity for the chosen reaction by itself but greatly enhances the activity when added to the existing catalyst. Iwasawa and co-workers used Sn-modified Rh catalysts for NO dissociation and NO–H_2 reaction [24]. They acknowledged that Sn metal has no significant catalytic activity by itself, because it does not interact with H_2, hydrocarbons, CO, or NO, but found that Sn can be used as a promoter for SiO_2-supported transition metal catalysts to enhance catalytic performance. Another possibility is that the addition of a second metal changes the morphology of the active metal. When one metal is deposited on another, one observes a number of different phenomena. The deposited metal may form islands on the substrate or may alloy into the first or deeper layers [25]. Although it was presumed that alloy formation was the essence of the promotional effect in bimetallic catalysts, more recent studies have shown that in some cases alloy formation is not desired. Waszczuk et al. [26] have found that a decorated Pt/Ru catalyst is twice as active for methanol electro-oxidation (in terms of current density and turnover frequency) as the commercial alloy catalyst, both of which have nominally identical Pt:Ru ratios. They concluded that ruthenium atoms present at the edge of Pt nano-sized islands display significantly enhanced activity for the CO poison removal compared with the active sites on a Pt/Ru alloy.

Consequently, it is important to characterise the size, structure, and distribution of the metal particles of these bimetallic catalysts in an attempt to understand the correlation between microstructure and catalytic properties. Characterisation of catalysts by the traditional bulk techniques can be very difficult because of the microscopic nature of the particles. This is especially true for bimetallic systems, which can be complicated by the presence of several metal phases [27]. For example, Rolison et al. [28] performed bulk and surface analyses of several commercial and industrial Pt–Ru/C electrocatalysts and highlighted the need to use a combination of techniques to characterise the catalysts; in particular, they found that X-ray diffraction (XRD) analysis on its own could give misleading results.

In this paper, Pt–Ru bimetallic catalysts are characterised by various techniques, including transmission electron microscopy (TEM), extended X-ray absorption fine structure (EXAFS) analysis, XRD, and X-ray photoelectron spectroscopy (XPS). The results of the characterisation are correlated with the activity of the catalysts for the hydrogenation of 2-butanone after a series of pretreatment procedures. Hydrogenation of 2-butanone was chosen as a test reaction primarily because the reaction is 100% selective to 2-butanol under mild conditions of temperature and pressure and thus allows comparison of activities of catalysts without complications due to selectivity.

2. Experimental

2.1. Catalyst preparation

The catalyst preparation method used depended primarily on whether the metals were impregnated onto the high-surface area graphite (HSAG) or activated carbon (AC) support. For the monometallic 5 wt% ruthenium/activated carbon catalyst, the wood-based activated carbon was slurried in deionised water, and an aqueous solution of Na_2RuO_4 was added. The slurry was allowed to cool and settle before being filtered and dried. A similar procedure was used to prepare the monometallic 1 wt% Pt/AC catalyst, using a Pt nitrate precursor. For the bimetallic AC-supported catalysts, the 5 wt% Ru/AC was used as the starting material. Aqueous solutions of the metallic nitrate precursor salts were allowed to contact the 5 wt% Ru/AC catalyst for 1 h before being dried in an oven overnight. The monometallic graphite-supported catalysts were prepared by making up the required solutions from chloride precursors. These salt solutions were added to the (HSAG) slurry, and reduced with formaldehyde or sodium hypophosphite. The catalysts were allowed to settle, then washed, filtered, and dried. A similar procedure was used to prepare the bimetallic HSAG-supported catalysts, except in this case a mixed solution of metal salts was made up and then added to the graphite slurry. Table 1 summarises details of the preparation procedures for all of the catalysts. It is important to note that in what follows, the term "fresh catalyst" refers to the catalyst state after drying the catalyst.

2.2. Catalytic tests

The hydrogenation reactions were performed in a 300 cm^3 Parr stainless steel autoclave with a maximum pressure of

Table 1
Summary of catalyst preparation variables

Metal loading	Metal precursor salts	Support	Reducing agent	Notation
5% Ru	Na_2RuO_4	Activated carbon	None	5Ru/AC
5% Ru 1% Rh	Na_2RuO_4 a nitrate of Rh	Activated carbon	None	5Ru1Rh/AC
5% Ru 1% Pd	Na_2RuO_4 a nitrate of Pd	Activated carbon	None	5Ru1Pd/AC
5% Ru 1% Pt	Na_2RuO_4 a nitrate of Pt	Activated carbon	None	5Ru1Pt/AC
5% Ru 2% Pt	Na_2RuO_4 a nitrate of Pt	Activated carbon	None	5Ru2Pt/AC
5% Ru 0.1% Pt	Na_2RuO_4 a nitrate of Pt	Activated carbon	None	5Ru0.1Pt/AC
5% Ru 0.5% Pt	Na_2RuO_4 a nitrate of Pt	Activated carbon	None	5Ru0.5Pt/AC
1% Pt	A nitrate of Pt	Activated carbon	None	1Pt/AC
5% Pt	Chloride	Graphite	Formaldehyde	5Pt/HSAG
4% Ru 1% Pt	Chlorides	Graphite	Sodium hypophosphite	4Ru1Pt/HSAG
1% Ru 4% Pt	Chlorides	Graphite	Sodium hypophosphite	1Ru4Pt/HSAG
5% Ru	Chloride	Graphite	Sodium hypophosphite	5Ru/HSAG

207 bar and a maximum temperature of 350 °C. For each experiment, 0.1 g of catalyst (particle size < 250 μm) was used to hydrogenate 2.4 g of 2-butanone diluted in 100 cm^3 of ultrapure water. The pressure was monitored by a pressure gauge on the removable head of the autoclave. The temperature was set using the temperature controller, which was connected to the heating mantle and monitored by a thermocouple located within the autoclave. A stirrer with a four-blade impeller rotating at approximately 1700 rpm was used to thoroughly mix the liquid in the vessel. A continuous supply of hydrogen from a fixed-volume reservoir was fed to the autoclave to maintain a constant pressure of 3 bar during the course of each reaction. The rate of hydrogen loss from the reservoir was monitored and logged continuously by means of a pressure transducer coupled to a PC. Given that hydrogen reacts stoichiometrically with 2-butanone to give 2-butanol as the only product (as confirmed by gas chromatography), hydrogen uptake was used as an indirect measure of the rate of reaction of 2-butanone. All hydrogenations were performed in duplicate at 30 °C.

In some cases the catalyst was pretreated in situ with 3 bar hydrogen before the reactant was added. Details of this pretreatment are as follows.

2.2.1. In situ pretreatment

For in situ pretreatment, 82 g water was added to 0.1 g catalyst and sealed in the autoclave. The vessel was flushed with nitrogen three times. The temperature was set to the desired level (60, 120, 180, or 230 °C) and was allowed to stabilise while the mixture was stirred slowly (approximately 150 rpm). Then 3 bar of hydrogen was introduced into the autoclave, and the catalyst was allowed to reduce for 90 min. The solution was then allowed to cool to 30 °C before being purged three times with nitrogen.

2.3. Scanning transmission electron microscopy

Small portions of catalyst sample were taken and crushed, then dusted onto a scanning transmission electron microscopy (STEM) grid (Cu). The samples were examined on a Tecnai F20 Transmission Electron Microscope operating at 200 kV. Approximately eight micrographs were recorded for each sample. The composition of selected nanoparticles was determined by energy-dispersive X-ray analysis. In this analysis, the electron probe beam was focused along a path containing regions of blank support and nanoparticles, X-ray fluorescence signals were collected at every nanometer along the path. The intensities of the signals characteristic of Pt and Ru were plotted against distance along the line scan.

2.4. Extended X-ray absorption fine structure

Data were collected at reaction temperature at the Synchrotron Radiation Source in Daresbury, U.K., using station 9.2. The spectra were recorded at the ruthenium K edge and the platinum L_{III} edge using a double-crystal Si(220) monochromator set at 50% harmonic rejection in transmission mode. Scans were collected and averaged using EXCALIB, which was also used to convert raw data into energy versus absorption data. EXBROOK was used to remove the background. The analysis of the EXAFS was performed using EXCURV98 on the raw data using the curved-wave theory. Phase shifts were derived from ab initio calculations using Hedin–Lundqvist exchange potentials and von Barth ground states. Comparisons were made with reference Ru and Pt foils and RuO_2 and PtO powders. The EXAFS analysis was performed as a function of catalyst reduction temperature using an in situ reaction cell with Kapton windows on a pressed pellet of catalyst with hydrogen gas. For the reoxidation treatment, the catalyst was purged with nitrogen before air was slowly admitted to minimise the risk of exotherms. The temperature was controlled with a Eurotherm PID controller with a thermocouple in contact with the catalyst.

2.5. X-Ray photoelectron spectroscopy

The samples were pressed and mounted on the specimen stage using double-sided adhesive tape and analysed with monochromatic Al-K_α radiation in a 500 μm spot at 150 W. The binding energies were all referenced to C1*s* at 284.8 eV. Detailed spectra were obtained at 40 eV pass energy.

2.6. X-Ray diffraction

XRD analysis was performed on a Siemens D5000 X-ray diffractometer with Cu-K_α radiation (1.5405 Å). In situ diffraction patterns were obtained using a home-built environmental cell as described previously [29]. For the reduction and oxidation treatments, hydrogen and air, respectively, were flowed over the sample at 20 $cm^3\ min^{-1}$, and the data were obtained at the treatment temperature.

2.7. Temperature-programmed reduction

Temperature-programmed reduction (TPR) experiments were performed with approximately 0.1 g of fresh catalyst in a Micromeritics Autochem 2910. The samples were placed in a U-shaped tube and cooled to −50 °C in argon. A high-purity mixture of 5% hydrogen in argon was fed in to the reactor, and the temperature was ramped up to 500 °C at a rate of 10 °C min. Hydrogen uptake, as monitored by a thermal conductivity detector (TCD), was recorded.

2.8. CO chemisorption

CO chemisorptions were performed using a Micromeritics Autochem 2910 to monitor CO uptake while pulsing CO over the catalyst at 4 °C. Approximately 0.1 g of catalyst was prereduced in 5% H_2/Ar for 120 min at 120 °C, then purged with He for 60 min before cooling to 4 °C. A mixture of 10% CO/He was pulsed into the reactor every 5 min, and the uptake as measured by the TCD was recorded. Pulsing continued until no further uptake of CO occurred. The CO peaks were integrated, and the total amount of CO chemisorbed was calculated. The pulse chemisorptions were repeated after reduction in 5% H_2/Ar at 180 and 230 °C.

3. Results

3.1. Catalytic activity

Various monometallic and bimetallic activated carbon-supported catalysts were prepared and tested for their activity for the hydrogenation of 2-butanone to 2-butanol. These results are summarised in Table 2. It was found that the addition of a second metal to Ru/AC catalysts resulted in enhanced activity for the liquid-phase hydrogenation of 2-butanone. This activity enhancement depended on the nature of the metal added. Platinum added as a second metal to ruthenium was found to produce a larger effect than either rhodium or palladium. In addition, it was found that there was an optimum concentration of platinum which, with the range of catalysts used in our work, was of the order of 1% Pt on a 5% Ru/AC catalyst. Concentrations of Pt above and below 1% gave catalysts with lower activity. It is noteworthy that Pt on its own had almost no activity for the reaction, and the arithmetic sum of the activities of the two monometallic 1Pt/AC and 5Ru/AC catalysts was less than half the activity of the bimetallic 5Ru1Pt/AC catalyst. This is clear evidence of a "bimetallic effect" in the hydrogenation of 2-butanone with platinum-promoted ruthenium catalysts.

Although activated carbon supports are frequently used in industry for liquid-phase hydrogenation reactions, there are problems associated with these supports. In particular, activated carbons are very heterogeneous materials, containing inorganic matter and numerous oxygen functional groups [30], making them difficult to characterise. Graphite is a much "cleaner" support. Therefore, to minimise problems with catalyst characterisation, it was decided to use graphite as well as activated carbon as supports for the bimetallic catalysts.

Table 2 shows that the graphite-supported 5Ru/HSAG catalyst was less active than the AC-supported counterpart. However, the HSAG catalysts showed the same trends as observed for the AC-supported materials. The 5Pt/HSAG catalyst had very low activity for the reaction, and (as in the case of the AC-supported catalysts) the combined rates of reaction over the two monometallic catalysts was less than half that obtained over the bimetallic 4Ru1Pt/HSAG catalyst. This is evidence of a "bimetallic effect" on the HSAG-supported catalysts. The bimetallic catalyst rich in Pt (1Ru4Pt/HSAG) had low activity for the reaction. However, if the rate was normalised to the number of Ru atoms in the catalyst, then the activity of the 1Ru4Pt/HSAG was significantly greater than that of the monometallic catalyst and approached that of the 4Ru1Pt/HSAG. This is an indication that the Ru in the 1Ru4Pt/HSAG had enhanced activity due to the "bimetallic effect," but there was a significant quantity of "free" Pt with low activity.

Table 2
Initial rates of reaction for a series of monometallic and bimetallic AC- and HSAG-supported catalysts

Catalyst	Rate of reaction (mmol kg^{-1} s^{-1})
5Ru/AC	364
5Ru1Rh/AC	665
5Ru1Pd/AC	438
5Ru1Pt/AC	850
5Ru0.1Pt/AC	403
5Ru0.5Pt/AC	499
5Ru2Pt/AC	643
1Pt/AC	2
5Ru/HSAG	168
4Ru1Pt/HSAG	459
1Ru4Pt/HSAG	104
5Pt/HSAG	29

Several authors [31–34] have studied the effect of different pretreatments on Ru-based catalysts, particularly for hydrogenolysis reactions [35,36], and have used their findings to characterise the nature of the active site. We used this approach to aid identification of the active site in our bimetallic catalysts for the hydrogenation of 2-butanone.

Fig. 1 clearly shows that hydrogen pretreatment of the catalyst had a sometimes dramatic effect on the catalyst activity. This effect was most noticeable in the bimetallic catalyst. The initial activity of the bimetallic catalyst was high and was slightly improved by exposure to hydrogen at 25 °C; however, in situ pretreatment in hydrogen at higher temperatures ($\geqslant$60 °C) resulted in drastically reduced activity, to the extent that after treatment at 230 °C, the catalyst was inactive for the reaction. Interestingly, when the catalyst was exposed to air (at 25 °C), there was significant recovery of catalyst activity after reduction at 230 °C. This demonstrates that treatment in oxygen can at least partially reverse the adverse effects of the reductive pretreatment in hydrogen. Reexposure of the catalyst to hydrogen at 230 °C after a cycle of reduction (at 230 °C) and oxidation (at 25 °C) resulted in decreased activity as compared with the activity of the catalyst after the oxidation step. However, the catalyst did retain some activity after this redox cycle, in contrast to the inactive catalyst obtained by a single pretreatment in hydrogen.

To investigate whether the activity reduction was due simply to the effects of temperature, the bimetallic catalyst was pretreated in nitrogen instead of hydrogen at 120 °C. Clearly, pretreatment in nitrogen had only a minor deactivating effect on the catalyst. This effectively means that a combination of temperature and hydrogen is necessary to deactivate the catalyst.

The behaviour of the monometallic 5Ru/HSAG subjected to the various pretreatments was quite similar to that observed for the bimetallic catalyst, with two notable exceptions. First, the monometallic catalyst was more resistant to deactivation by reductive treatment and was deactivated only after reduction in hydrogen at 180 °C. The initial catalyst activity (with no pretreatment) could be recovered by exposure to air after reduction at 230 °C. Second, the bimetallic catalyst showed very little difference between the activity of the fresh catalyst and that of the catalyst exposed to in situ hydrogen pretreatment at 25 °C, whereas for the 5Ru/HSAG catalyst, H_2 pretreatment at 25 °C resulted in a noticeable increase in activity. The unchanged activity of the 4Ru1Pt/HSAG catalyst after H_2 pretreatment at 25 °C was expected. EXAFS analysis (Tables 4 and 5) show that the catalyst was fully reduced at 25 °C and likely reduced

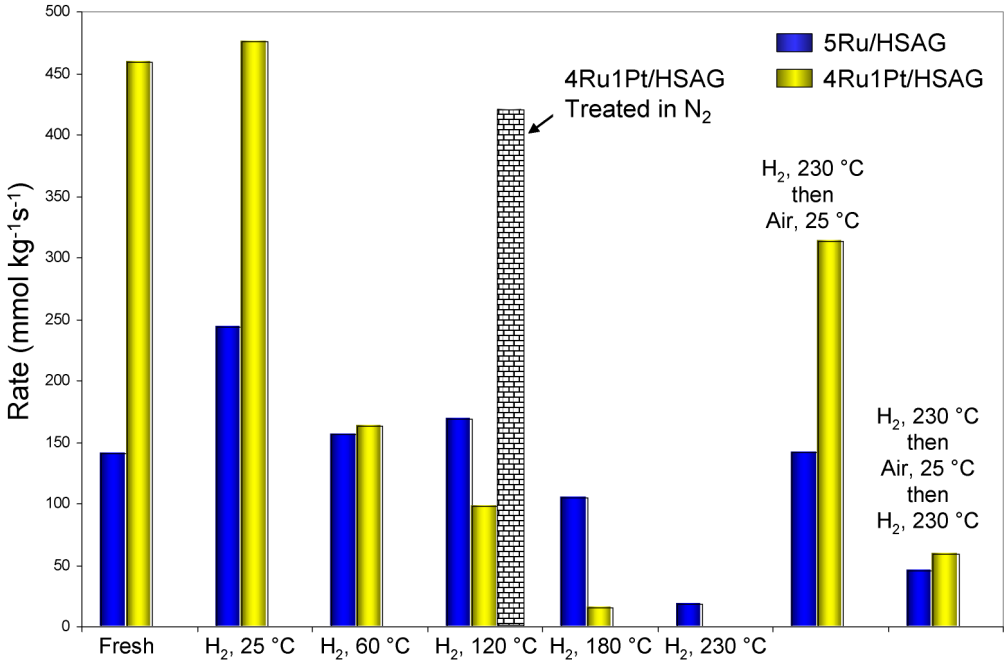

Fig. 1. Comparison of average rates of hydrogenation of 2-butanone with 5Ru/G and 4Ru1Pt/G with various in situ pre-treatments. Note: Both catalysts have been chemically reduced during preparation.

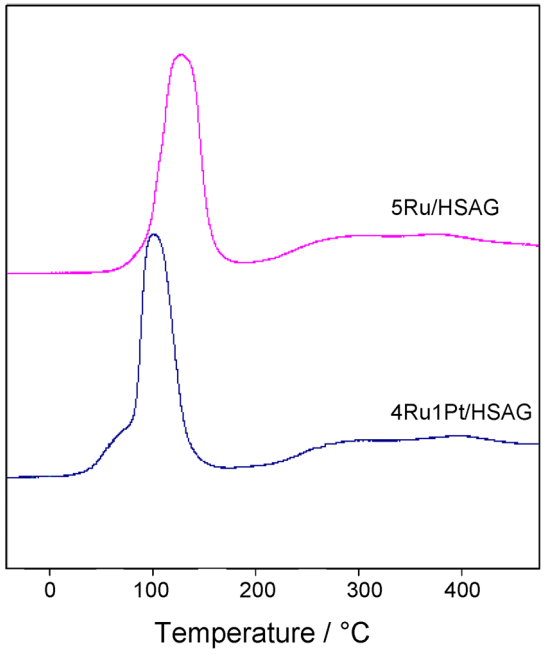

Fig. 2. TPR of the 5Ru/HSAG and 4Ru1Pt/HSAG catalysts.

very quickly under reaction conditions at 30 °C. Therefore, the catalyst states after in situ prereduction in H_2 at 25 °C and under reaction conditions are likely to be very similar. For the 5Ru/G catalyst, EXAFS and TPR analysis (Fig. 2) show that the catalyst exhibited no bulk reduction at 25 or 30 °C. However, XPS analysis (Table 7) indicated that Ru^{4+} and Ru^{6+} species were present on the 5Ru/HSAG surface, whereas TPR analysis showed that the average oxidation state of the Ru (bulk and surface) was Ru^{4+}. This means that the surface of the catalyst was more oxidized than the bulk; thus, it is possible that the surface was partially reduced (e.g., from Ru^{6+} to Ru^{4+}) by hydrogen treatment at 25 °C. That no peaks associated with the partial reduction were observed on TPR analysis may be because reduction occurs at a lower temperature than the starting temperature of the TPR. This partial reduction of the surface may be sufficient to promote catalyst activity.

It should be noted that very similar effects were also found for monometallic ruthenium and bimetallic ruthenium/platinum catalysts supported on AC. The effects of the pretreatments on the catalyst activity are not readily explainable and may possibly be attributed to such effects as changes in the dispersion or morphology of the catalysts and changes in the oxidation state. In the case of the bimetallic catalyst, changes in the distribution and bonding of the two metals on the surface of the catalyst could be factors. To gain a clearer understanding of the nature of the active site on these catalysts, the 5Ru/HSAG and 4Ru1Pt/HSAG catalysts were characterised using a number of different techniques.

3.2. Catalyst characterisation

3.2.1. CO chemisorption

CO chemisorption was carried out over the 5% Ru/HSAG catalyst at three different reduction temperatures. Analysis of CO uptake after prereduction at temperatures of 120–230 °C showed that CO uptake remained constant (Table 3), indicating that no sintering of the Ru particles occurred at temperatures up to 230 °C.

3.2.2. Temperature-programmed reduction

The TPR profile of the monometallic 5Ru/HSAG catalyst showed one main reduction peak at 128 °C, which can be attributed to the reduction of ruthenium oxide (Fig. 2). Quan-

Table 3
Total CO uptake on 5% Ru/HSAG during CO pulse chemisorptions

Reduction temperature (°C)	CO/Ru molar ratio
120	0.32
180	0.34
230	0.34

tification of hydrogen consumption during TPR corresponded to the reduction of Ru^{4+} to Ru^0. This demonstrates that even subjecting the catalyst to a reduction treatment with formaldehyde or sodium hypophosphite during catalyst preparation was not sufficient to keep the final catalyst in a reduced state. TPR analysis of the bimetallic catalyst revealed two peaks, a main peak at 100 °C and a shoulder peak at 70 °C. The peak at 100 °C can be attributed to the reduction of Ru^{4+}, and that at 70 °C can be attributed to the reduction of Pt, probably PtO. The presence of Pt in the bimetallic catalyst lowered the temperature of reduction of ruthenium oxide in the bimetallic catalyst compared with the monometallic 5Ru/HSAG catalyst. The small broad peak starting at 200 °C in both TPR profiles can be attributed to methanation of CO or CO_2 formed from decomposition of surface oxygen groups on the support [37].

3.2.3. *X-Ray diffraction*

XRD analysis was performed on the 5Ru/HSAG and 4Ru 1Pt/HSAG catalysts reduced at different temperatures. No peaks due to crystalline Ru or RuO_2 were observed in either the monometallic or bimetallic catalysts. In the case of the Ru/G, this indicates that the Ru was present in a highly dispersed form, with particle sizes below the detection limit of the technique (<4 nm). In the case of the bimetallic catalyst, the absence of Ru or RuO_2 crystallites suggests that the Ru was highly dispersed. This could be in the form of Ru, as part of a PtRu ensemble, or even as a PtRu alloy. Broad peaks due to Pt (or possibly a Pt alloy) were observed corresponding to a particle size of 4 nm; however, little change was observed as a function of temperature or atmosphere.

3.2.4. *Scanning transmission electron microscopy*

STEM coupled with energy-dispersive X-ray (EDX) analysis was used to obtain information on the nature of the particles on the fresh monometallic and bimetallic catalysts. Fig. 3 shows that the Ru exists primarily as clusters of Ru particles of 1–3 nm in diameter. Likewise, Fig. 4 shows that the particles of the 4Ru1Pt/HSAG catalyst also exist primarily in the form of clusters of small particles (1–2 nm). The compositions of individual particles were determined by atom-probe EDX analysis. EDX spectra were collected at regular intervals of 1 nm as the beam moved along the line indicated in the dark-field image in Fig. 5. This 30 nm-long line scan incorporates one full cluster and portions of another two clusters interdispersed on the graphite support. The fluorescence intensity for Ru and Pt, together with the background fluorescence, were plotted as a function of distance along the scan length. Fig. 6 clearly shows that the clusters contained a mixture of Pt and Ru atoms. After subtracting the background, it was found that for the cluster en-

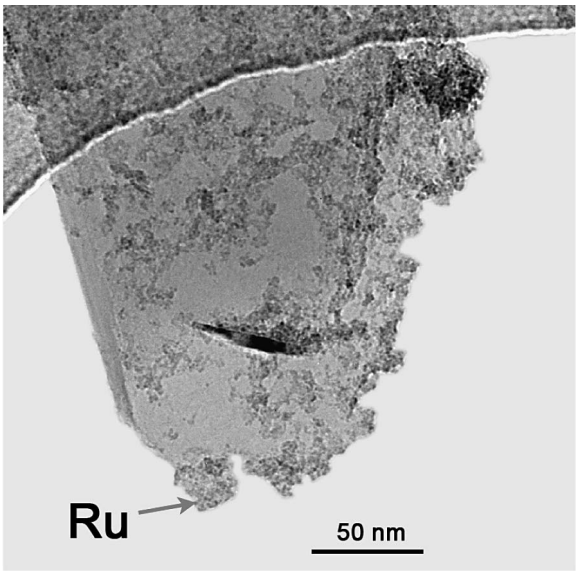

Fig. 3. TEM of the 5Ru/HSAG catalyst.

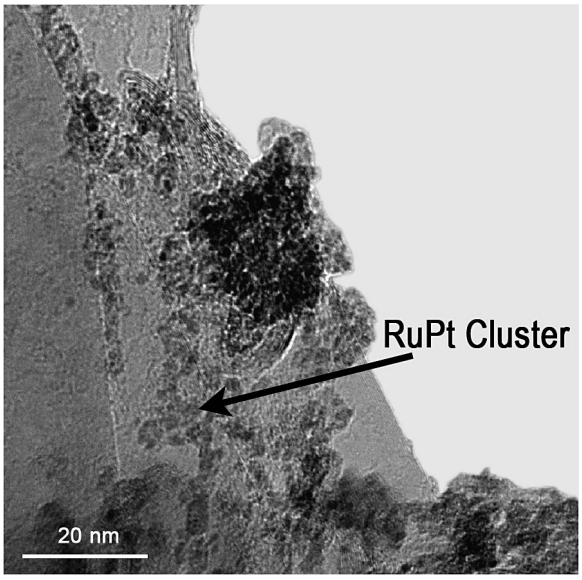

Fig. 4. TEM of the 4Ru1Pt/HSAG catalyst.

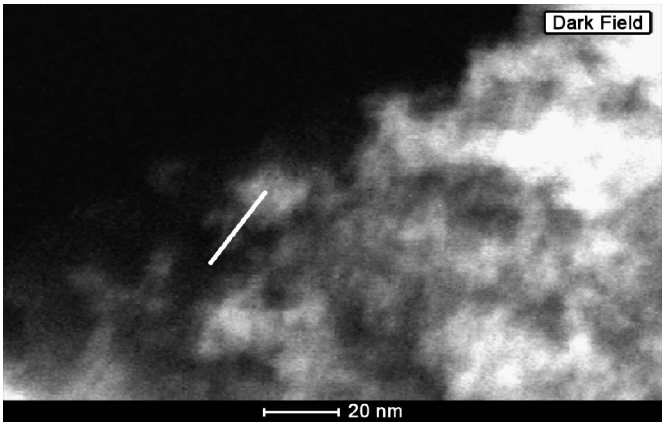

Fig. 5. TEM dark field image of 4Ru1Pt/HSAG sample.

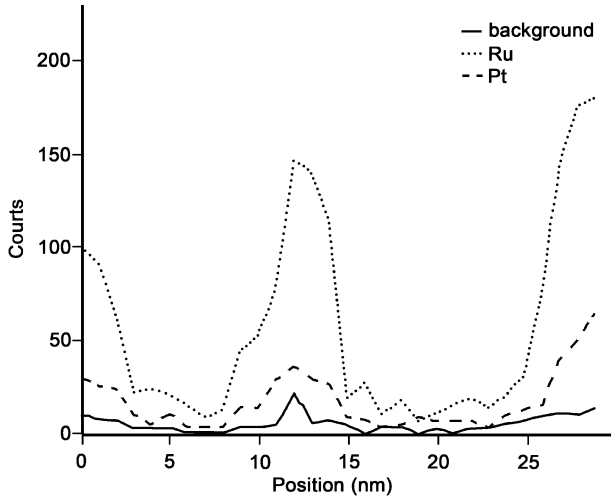

Fig. 6. Plot of fluorescence intensities obtained from EDX analysis during the line scan represented by the white line in Fig. 4.

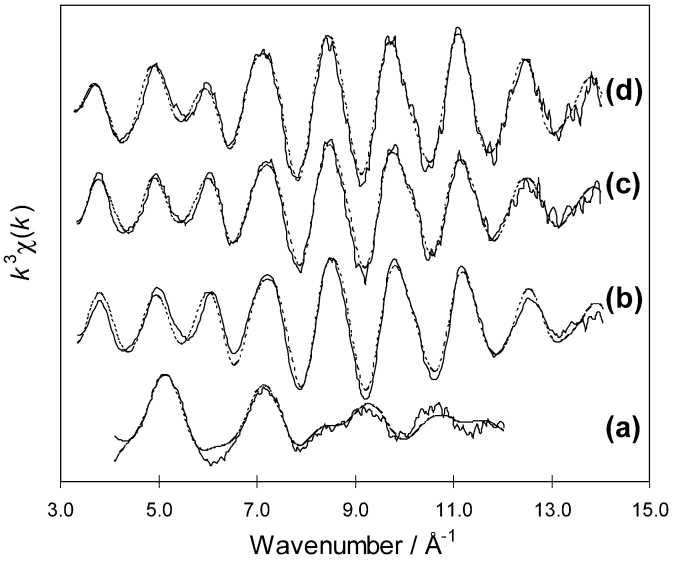

Fig. 7. Raw $k^3\chi(k)$ EXAFS data from the Ru K-edge of 4Ru1Pt/HSAG under different reaction conditions: (a) fresh catalyst, (b) following reduction at room temperature, (c) following reduction at 230 °C and (d) after reduction and re-exposure to air at room temperature.

countered between 8 and 15 nm along the scan path, the atomic ratio of Ru:Pt was 4.7:1. This is lower than the bulk atomic ratio of Ru:Pt in the catalyst (7.8:1). However, because this is a measurement from only one cluster, it is not possible to draw any conclusions about the average ratio of the metals in the particles of the catalyst. The important point is the existence of bimetallic clusters.

3.2.5. *Extended X-ray absorption fine structure*

Figs. 7–10 show the EXAFS and pseudoradial distribution functions for the Ru K-edge and Pt L_{III}-edge of the 4Ru1Pt/HSAG catalyst as functions of different pretreatments. EXAFS analysis was also performed on the 5Ru/HSAG and 5Pt/HSAG catalysts. For both of the fresh Ru-containing catalysts, the ruthenium K-edge data showed the presence of oxygen coordination consistent with bond distances found in

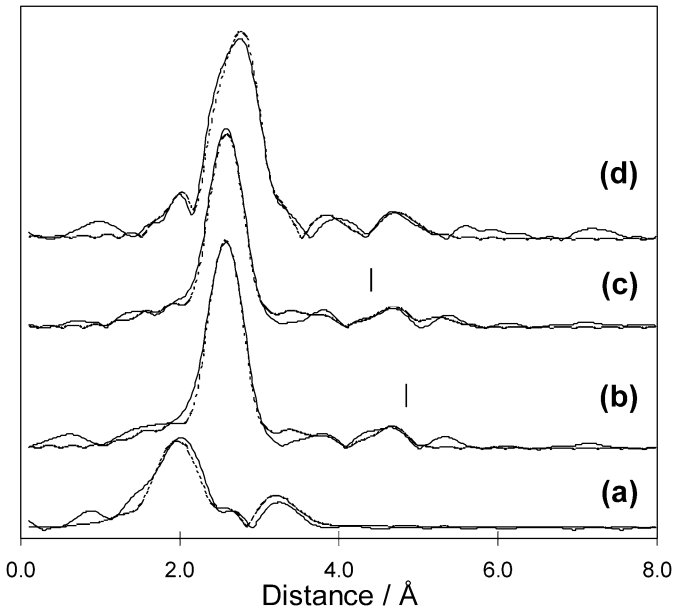

Fig. 8. Comparison of the experimental (solid line) and fitted (dashed line) *pseudo* radial distribution functions of the Ru K-edge of 4Ru1Pt/HSAG under different reaction conditions: (a) fresh catalyst, (b) following reduction at room temperature, (c) following reduction at 230 °C and (d) after reduction and re-exposure to air at room temperature.

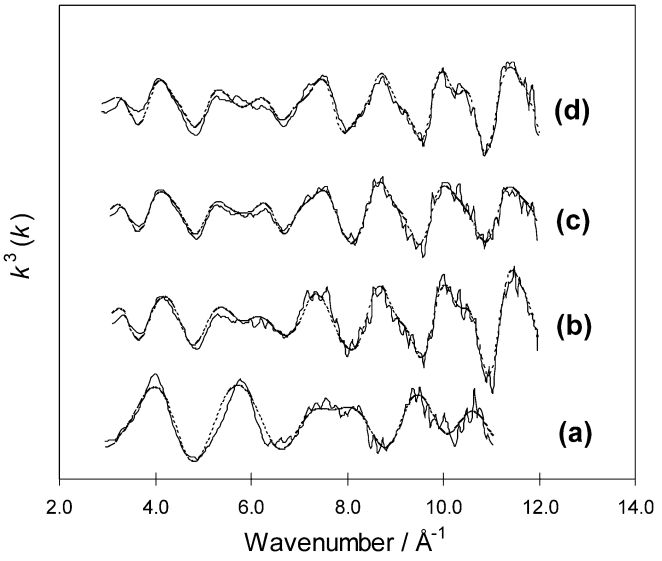

Fig. 9. Raw $k^3\chi(k)$ EXAFS data from the Pt L_{III}-edge of 4Ru1Pt/HSAG under different reaction conditions: (a) fresh catalyst, (b) following reduction at room temperature, (c) following reduction at 230 °C and (d) after reduction and re-exposure to air at room temperature.

RuO_2. This is as expected, considering that the TPR results (Fig. 2) showed that even though these catalysts were subjected to chemical reduction during catalyst preparation, they were readily oxidised by exposure to the lab atmosphere before EXAFS analysis. Table 4 summarises the parameters used to fit the EXAFS data. In agreement with TPR results, in the absence of platinum, little reduction of the ruthenium was observed below 120 °C. At 120 °C, reduction to ruthenium metal was observed with no evidence of oxygen coordination and a ruthenium first shell coordination number of 6.9, indicating an

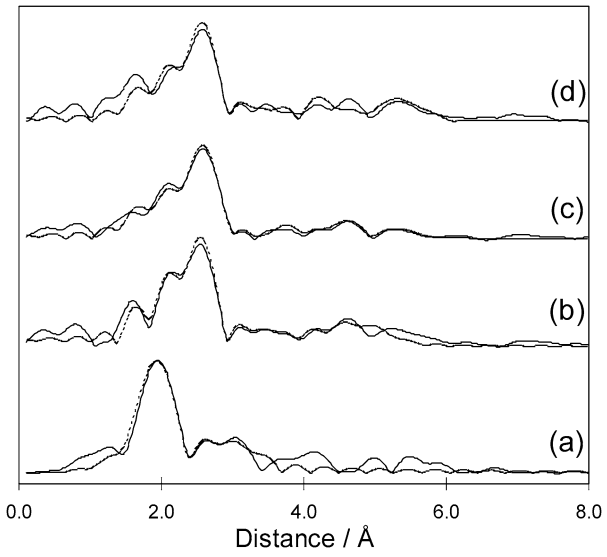

Fig. 10. Comparison of the experimental (solid line) and fitted (dashed line) *pseudo* radial distribution functions of the Pt L_{III}-edge of 4Ru1Pt/HSAG under different reaction conditions: (a) fresh catalyst, (b) following reduction at room temperature, (c) following reduction at 230 °C and (d) after reduction and re-exposure to air at room temperature.

Table 4
Structural parameters from the fitted EXAFS spectra for the Ru K-edge of 4Ru1Pt/HSAG and 5Ru/HSAG

Catalyst/ treatment	Shell/ atom	Shell distance (Å)	Co-ordination number	Debye–Waller factor (Å)	Fit factor (%)
4Ru1Pt/HSAG (fresh)	1 O	1.98	4.5	0.017	28.9
	2 Ru	3.11	5.4	0.033	
4Ru1Pt/HSAG (reduced at 25 °C)	1 Ru	2.65	6.9	0.017	25.7
	2 Ru	3.75	3.3	0.027	
	3 Ru	4.65	2.6	0.014	
4Ru1Pt/HSAG (reduced then reexposed to air)	1 O	2.00	3.0	0.012	20.2
	2 Ru	2.67	6.2	0.014	
	3 Ru	3.78	2.4	0.019	
	4 Ru	4.73	3.1	0.013	
5Ru/HSAG (fresh)	1 O	1.98	4.5	0.016	26.5
	2 Ru	3.11	4.5	0.030	
5Ru/HSAG (reduced at 120 °C)	1 Ru	2.66	6.2	0.015	25.1
	2 Ru	3.77	3.0	0.022	
	3 Ru	4.55	3.3	0.017	
5Ru/HSAG (reduced then reexposed to air)	1 O	2.00	2.3	0.025	18.6
	2 Ru	2.68	6.9	0.015	
	3 Ru	3.78	1.8	0.013	
	4 Ru	4.68	3.8	0.014	

average metal cluster size of ∼1 nm. Further increases in the reduction temperature up to 230 °C produced no change in the EXAFS data. Furthermore, exposure to air after reduction only caused a small amount of reoxidation. Oxygen coordination could be fitted at a distance of ∼2 Å; however, the majority of the ruthenium showed Ru–Ru coordination at ∼2.7 Å, due to metallic ruthenium. In the presence of platinum, reduction of the catalyst in a flow of H_2 and formation of metallic ruthenium was observed at room temperature. As with the monometallic

Table 5
Structural parameters from the fitted EXAFS spectra for the Pt L_{III}-edge of 4Ru1Pt/HSAG and 5Pt/HSAG

Catalyst/ treatment	Shell/ atom	Shell distance (Å)	Co-ordination number	Debye–Waller factor (Å)	Fit factor (%)
4Ru1Pt/HSAG (fresh)	1 O	1.98	3.3	0.013	33.2
	2 Ru	2.63	0.5	0.014	
	3 Pt	2.72	2.1	0.010	
4Ru1Pt/HSAG (reduced at 25 °C)	1 Ru	2.69	3.7	0.011	32.7
	2 Pt	2.74	4.9	0.015	
	3 Ru	3.78	0.6	0.004	
	4 Pt	3.82	2.6	0.016	
	5 Ru	4.69	0.8	0.007	
	6 Pt	4.81	2.0	0.003	
4Ru1Pt/HSAG (reduced then reexposed to air)	1 Ru	2.70	3.6	0.013	35.7
	2 Pt	2.75	4.8	0.018	
	3 Ru	3.79	1.1	0.009	
	4 Pt	3.85	1.3	0.004	
	5 Ru	4.73	1.9	0.011	
	6 Pt	4.82	1.9	0.002	
5Pt/HSAG (fresh)	1 O	2.01	1.3	0.008	25.7
	2 Pt	2.76	5.0	0.011	
	3 Pt	3.61	1.1	0.013	
	4 Pt	4.80	4.3	0.016	
5Pt/HSAG (reduced at 25 °C)	1 Pt	2.76	9.0	0.013	20.7
	2 Pt	3.90	3.9	0.015	
	3 Pt	4.80	13.6	0.019	
	4 Pt	5.43	6.2	0.013	

catalyst, no further change was observed with increasing reduction temperature, and on reexposure to air, a small degree of oxidation was observed, implying only surface reoxidation. It should be noted that although a Ru–Pt could be fitted to the Ru K-edge data for the bimetallic catalyst after reduction, examination of the χ^2 statistical tests demonstrated that the shell was not significant.

Examining the Pt L_{III}-edge data for the fresh monometallic and bimetallic catalyst (Figs. 9 and 10) similarly showed oxygen coordination; however, in contrast with the ruthenium, a significant amount of Pt–Pt coordination was also present. In the bimetallic sample, some (albeit small) ruthenium coordination around the platinum was observed. Both of the platinum catalysts showed complete reduction at room temperature, in agreement with the Ru K-edge data for the bimetallic catalyst. There was no change in the EXAFS data as a function of reduction temperature. The 5Pt/HSAG catalyst contained large metal particles with first shell coordination number 9, indicating a particle size of ∼2.5 nm assuming hemispherical particles. For the bimetallic catalyst, the Pt L_{III}-edge data clearly showed both Pt–Pt and Pt–Ru coordination, with more Pt–Pt coordination than Pt–Ru coordination. Table 5 summarises the parameters used to fit the Pt L_{III}-data. No oxygen coordination was observed on reexposure to air.

It is clear that the Pt–Ru coordination observed in the Pt L_{III}-edge data is not mirrored by complementary coordination in the Ru K-edge data. Coupled with the fact that the average Ru coordination number indicates a particle size of ∼1 nm, this

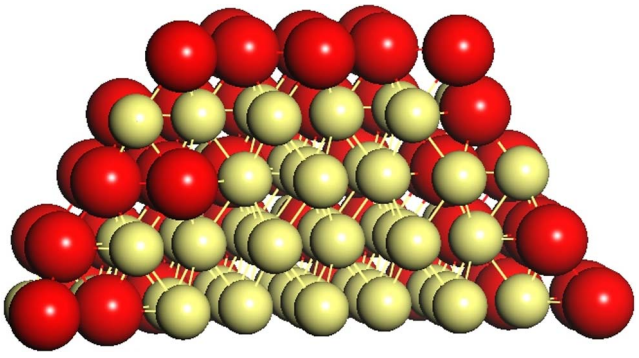

Fig. 11. Cross-section of bimetallic RuPt cluster (Pt atoms, Ru atoms).

Table 6
Model co-ordination numbers for a 1:1 Pt–Ru hemisphere containing a 1.1 nm Ru core and two layers of randomly mixed Pt–Ru overlayers with 66% Ru in the inner layer and 13% Ru in the outer layer

Atom type	Co-ordination number
Pt–Pt	4.4
Pt–Ru	3.5
Ru–Ru	6.7

suggests that at least two types of particles are present in the reduced bimetallic sample. The data are consistent with the coexistence of monometallic Ru particles and mixed metal particles. Possible structures can be examined using geometric models of the bimetallic clusters. One model that is consistent with the data comprises a PtRu bimetallic particle with a 1:1 stoichiometry, with a ruthenium core of approximately 1.1 nm and two mixed layers of Pt and Ru at the surface, with the outermost mixed layer enriched in Pt. The total dimension of the particle in this model is 2.0 nm. Fig. 11 shows the cluster proposed with the proportion of atoms in each section. Table 6 also gives the theoretical coordination numbers associated with this cluster, which, given an error of at least ±0.5 in the coordination number, are in good agreement with the experimentally determined values from the Pt L_{III}-edge data. A 1:1 Pt:Ru ratio for the bimetallic particles would indicate that 75% of the Ru was found in the monometallic form, a result consistent with the absence of a significant Ru–Pt shell for the Ru K-edge data.

3.2.6. X-Ray photoelectron spectroscopy

XPS analysis was performed on the 5Ru/HSAG, 4Ru1Pt/HSAG, and 5Pt/HSAG catalysts. Table 7 gives the binding energies of the Pt4$f_{7/2}$ and Ru3$d_{5/2}$ peaks as a function of treatment. In the fresh 4Ru1Pt/HSAG catalysts, the platinum was oxidised with binding energy at 72.8 eV attributable to Pt^{2+} [7]. In addition, a peak was observed at 76.0 eV, likely associated with Pt^{4+}; although this binding energy is higher than is normally associated with the 4+ oxidation state (∼74.7 eV), this may be due to interactions of Pt with ruthenium oxide, as reported by Villulas et al. [38]. The spectrum for Ru 3d was deconvoluted into two components with binding energies of 281.5 and 282.7 eV. The peak at 281.5 eV can be attributed to Ru^{4+} [38,39], and that at 282.7 eV can be attributed to either Ru^{6+} or hydrous speciation of Ru [28,40]. A similar Pt/Ru atomic ratio of 0.14 was found by both XPS and inductively coupled plasma-AES analysis indicating no preferential surface segregation. After reduction in situ at 230 °C for 1 h, the Ru was completely reduced to Ru (0), as indicated by the peak at 280.1 eV [28,38]. For Pt, a single peak at 72.0 eV was evident after reduction at 230 °C; this can be attributed to Pt metal [38]. A significant increase in the Pt/Ru ratio as determined by XPS was observed on reduction, indicating surface segregation of the platinum. This is in agreement with the EXAFS results.

Table 7
XPS characterisation data for Ru/G, 4Ru1Pt/G and 5Pt/G catalysts

Catalyst/ treatment	Binding energy (eV) (at%)		Pt/Ru atomic ratio	
	Pt4$f_{7/2}$	Ru3$d_{5/2}$	XPS	Bulk
4Ru1Pt/HSAG (fresh)	72.8 (60) 76.0 (40)	281.5 282.7	0.14	0.14
4Ru1Pt/HSAG (reduced at 230 °C)	72.0	280.1	0.4	0.14
4Ru1Pt/HSAG (reduced then re-exposed to air)	71.9 (66) 73.3 (33)	280.3	0.5	0.14
5Ru/HSAG (fresh)		281.5 282.8		
5Pt/HSAG (fresh)	71.5 (68) 72.6 (32)			

In the monometallic ruthenium catalyst, oxidised ruthenium was observed with both Ru^{4+} and Ru^{6+} oxidation states present, as found in the bimetallic catalyst. In contrast, the monometallic platinum catalyst showed a much higher degree of reduction compared with the bimetallic catalyst with both Pt^0 and Pt^{2+} present. These trends for the fresh 5Ru/HSAG and 5Pt/HSAG catalysts are in agreement with the EXAFS analysis, where metal–metal coordination was observed only in the 5Pt/HSAG fresh catalyst, indicating that in the 5Ru/HSAG catalyst, the ruthenium was fully oxidised and showed no metallic character.

4. Discussion

RuPt bimetallic catalysts are particularly active for the hydrogenation of 2-butanone to 2-butanol. The optimum loading of Pt in our experiments was 1%. Catalysts with loadings higher or lower than 1% demonstrated lower activities. Given that Pt has a very low activity for the hydrogenation reaction, it is reasonable to speculate that high loadings of Pt will tend to cover or encapsulate active Ru particles, thus rendering the catalyst less active. At low Pt loadings (<1%), there may be insufficient Pt in contact with Ru to create a sufficient number of bimetallic particles of the correct stoichiometry or morphology. Indeed, it is evident that as the Pt loading decreases from 1%, the catalyst activity approaches that of the monometallic Ru catalyst.

RuPt catalysts supported on graphite were less active than their carbon-supported counterparts but followed similar kinetic trends as those for the carbon-supported materials. The 4Ru1Pt/HSAG catalyst was the most active, considerably more active than the sum of the activities of the monometallic cata-

lysts. STEM analysis of the fresh Ru/HSAG and 4Ru1Pt/HSAG catalysts showed that the catalysts consisted primarily of clusters of small particles (1–3 nm) residing on the support. EDX analysis of particles on the 4Ru1Pt/HSAG catalyst confirmed that the clusters were bimetallic, ruling out the possibility of exclusively segregated Ru and Pt particles. EXAFS analysis showed that the particles within the clusters were bimetallic and that the average particle size in both the 5Ru/HSAG and 4Ru1Pt/HSAG catalysts was 1–2 nm.

The EXAFS data also revealed that there must be two types of particle on the surface of the bimetallic 4Ru1Pt/HSAG catalyst: bimetallic RuPt particles and monometallic Ru particles, both of the order of 1–2 nm. For the bimetallic particles, it is possible to fit the data with a model in which a Ru core (1.1 nm) is enclosed with two mixed Pt-rich layers, with the outer layer containing only 13 at% Ru. Surface enrichment by Pt was also confirmed by XPS analysis and is consistent with theoretical calculations performed by Ruban et al. [41]. They have investigated the general trends in the surface segregation phenomena in transition metal alloys. Their matrix of results indicates that Ru and Pt will strongly segregate from each other and that in Ru-rich catalysts, Pt will segregate to the surface of the Ru particles.

In situ EXAFS analysis of the 5Ru/HSAG and 4Ru1Pt/HSAG at room temperature and during exposure to hydrogen at different temperatures revealed that the bimetallic catalyst was readily reduced by exposure to hydrogen at room temperature. However, reduction of the 5Ru/HSAG catalyst required a temperature $>60\,^{\circ}C$.

The effect of different pretreatment temperatures on catalyst activity showed some interesting trends. For the 4Ru1Pt/HSAG catalyst, there was clearly a trend of decreasing activity with increasing temperature of in situ reduction. After reduction at 230 °C, the catalyst was almost totally inactive. The results of CO chemisorptions on the 5Ru/HSAG and coordination numbers extracted from EXAFS experiments on both the 5Ru/HSAG and 4Ru1Pt/HSAG catalyst clearly showed no change in the metal particle sizes on reduction at temperatures up to 230 °C. This is in agreement with the findings of Bond et al. [35], who used EXAFS and H_2 and CO chemisorption to show that Ru did not sinter even when treated in H_2 up to a temperature of 480 °C.

Miura et al. [8] found that heat treatments in H_2 at 477 and 627 °C resulted in a sharp drop in the Ru surface composition of their Pt/Ru/SiO_2 bimetallics, even though the total number of particles remained constant. They also found that excessive Pt at the surface was detrimental to the activity of their catalysts for the hydrogenation of benzene. XPS analysis of the 4Ru1Pt/HSAG catalyst showed that treatment at 230 °C in H_2 resulted in surface enrichment by Pt compared with the fresh material. However, surface enrichment by Pt cannot be used as an explanation for the decreased activity of our catalysts with increasing temperature of reduction. First, the EXAFS spectra remained constant with changing temperature of reduction, ruling out any further enrichment by Pt after the initial reduction at room temperature. Second, the monometallic 5Ru/HSAG catalyst also showed a trend of decreased activity with increasing temperature of hydrogen pretreatment. Clearly, this cannot be attributed to enrichment by platinum, thus indicating that some other process must be responsible for deactivation of the catalysts.

Interestingly, heat treatment in N_2 had no effect on the activity, indicating that hydrogen is necessary for deactivation of the catalyst. It was also found that the activity could be mostly recovered and enhanced by exposure of the catalyst to oxygen at room temperature. This was found to be true of both the monometallic and bimetallic catalysts.

These results find some resonance in the findings of Bond et al. [36] that for the gas-phase hydrogenolysis of ethane over a 1% Ru/Al_2O_3 catalyst, a low-temperature oxidative treatment of the catalyst caused a significant increase in catalyst activity. In addition, they also found that a high-temperature treatment in hydrogen resulted in significantly decreased activity. The high-temperature treatment did not result in a change in Ru dispersion, so they speculated that the oxidative treatment could create a higher proportion of active Ru^{x+} ions, which could be removed by high-temperature hydrogen treatment. Alternatively (and more plausibly), they suggested that the oxidation treatment could cause structural changes in Ru particles, increasing the number of active defect sites. These defects would be removed on heating to high temperatures in hydrogen. Reversible structural changes were clearly observed by Schmidt and co-workers [33,42] during successive oxidation–reduction treatments over various catalysts. They noted that high activity associated with oxidation and low-temperature reduction was related to the ability to maintain low-coordination, high-reactivity (defect) sites.

The differences in activity caused by pretreatment of the 4Ru1Pt/HSAG catalyst in N_2 rather than in H_2 at 120 °C can also most likely be explained by morphological changes. Wang et al. [43] found that annealing Pt particles in H_2 at 600 °C produced predominantly cube-shaped particles, exposing mostly (100) planes, whereas heating these cubes in N_2 at the same temperature caused the shapes to change to spheres, exposing additional planes. The temperatures used by Wang et al. are clearly much higher than those used in our study. However, for the bimetallic catalyst, a temperature of 120 °C may be sufficient to cause smoothing of the particle surface, leading to loss of defect sites. Lauth et al. [44] demonstrated that the Ru $(10\bar{1}0)$ surface can undergo surface reconstruction under hydrogen at low temperatures.

The experimental data for the effect of pretreatment on activity of the Ru monometallic catalysts seem to indicate that the hydrogenation of 2-butanone is a structure-sensitive reaction. In view of reports cited above that indicate the importance of the surface roughness (surface defect concentration) of Ru catalysts, we conclude that the activity variations observed for the hydrogenation of 2-butanone on Ru catalysts reduced at different temperatures is due to a gradual smoothing of the surface. An alternative, possibly related effect could be the enhanced chemisorption of hydrogen on defect sites. Lauth et al. [44] noted that hydrogen adsorption on atomically "rough" Ru surfaces is facile, with H_2 having a high sticking probability. This is not the case for many "smooth" low-index transition metal

surfaces, where adsorption is often an activated process resulting in low sticking probabilities. These authors noted that surface defects, or centres of roughness, were particularly important for the dissociative adsorption of H_2. It is interesting to note that H_2 pretreatment at temperatures above 25 °C has a much greater detrimental effect on the activity of the bimetallic catalyst than the 5Ru/HSAG. The EXAFS results show that this cannot be attributed to greater segregation of inactive Pt to the surface. It appears that in this case the process of surface smoothing and loss of activity could be enhanced by the presence of Pt.

Pt has a significant effect on the activity of Ru for the hydrogenation of 2-butanone. EXAFS and XPS consistently show that Ru and Pt are combined into bimetallic clusters. The method of catalyst synthesis has not yet been perfected, and so monometallic Ru and Pt particles are also likely present. However, the fact that the activities of the bimetallic catalysts at 1% Pt loading are much greater than the arithmetic sum of the activities of the individual metals suggests a true synergy between bimetallic Ru and Pt. Modeling calculations suggest that Pt will be enriched in the surface of Ru/Pt bimetallic particles, so the logical explanation for the effect of Pt is to modify the Ru surface. This could occur because the Pt breaks up the ensembles of Ru atoms, but would require that the Pt be located in rather than on the Ru surface. The fact that Ru and Pt tend to segregate might make this unlikely.

On the other hand, clusters of Pt atoms on the Ru surface could provide sites for dissociative adsorption of H_2. If this were a rate-determining process, particularly in the context of competitive adsorption between H_2 and 2-butanone, then the Pt could facilitate the hydrogenation reaction. In this respect, the role of Pt would be comparable to surface roughening in the case of monometallic Ru.

5. Conclusion

RuPt bimetallic carbon-supported catalysts are particularly active for the hydrogenation of 2-butanone to 2-butanol. A ratio of 5 wt% Ru:1 wt% Pt on AC was found to be optimum; catalysts with lower or higher ratios were less active. The activity of the 5Ru1Pt/AC bimetallic catalyst was more than double that of the sum of the activities of the monometallic 5Ru/AC and 1Pt/AC catalysts, providing evidence of a “bimetallic” effect. Similar results were obtained on HSAG-supported catalysts. Pretreatment of the monometallic and bimetallic catalysts in hydrogen had a significant effect on the activity. There was a general trend of decreased activity of the bimetallic and monometallic Ru-based catalysts with increasing temperature of prereduction in hydrogen. This loss of activity was almost fully reversible by exposing the catalysts to air after reduction. The changing activity with exposure to different gas-phase environments cannot be attributed to changes in particle size or surface composition; instead, we propose that defect sites are most active for the reaction and that the introduction of hydrogen results in a gradual smoothing of the surface and loss of defect sites. This process is reversible on the introduction of air.

TEM coupled with EDX analysis of the bimetallic catalysts revealed that they consisted of clusters of particles of the order of 1–2 nm. EXAFS analysis showed two types of particles on the surface of the bimetallic 4Ru1Pt/HSAG: monometallic Ru and bimetallic RuPt particles. For the bimetallic particles, it was possible to fit the data with a model in which a Ru core of 1.1 nm is enclosed by two Pt-rich layers, with the outer layer containing only 13 at% Ru.

Acknowledgments

We thank Johnson Matthey, PLC for financial support for this project, Peijun Hu for useful discussions on modeling the EXAFS data, and Tony Busby (Johnson Matthey) for the XPS and TEM analyses.

References

[1] V.D. Stytsenko, Appl. Catal. A 126 (1995) 1.
[2] R. Burch, J. Catal. 71 (1981) 348.
[3] P. Lu, T. Teranishi, K. Asakura, M. Miyake, N. Toshima, J. Phys. Chem. B 103 (1999) 9673.
[4] J.C. Davies, B.E. Hayden, D.J. Pegg, Surf. Sci. 467 (2000) 118.
[5] K.A. Friedrich, K.P. Geyzers, U. Linke, U. Stimming, J. Stumper, J. Electroanal. Chem. 402 (1996) 123.
[6] W. Rachmady, M.A. Vannice, J. Catal. 209 (2002) 87.
[7] Y. Hara, K. Endou, Appl. Catal. A 239 (2003) 181.
[8] H. Miura, H. Taguchi, K. Sugiyama, T. Matsuda, R.D. Gonzalez, J. Catal. 124 (1990) 194.
[9] K. Tahara, E. Nagahara, Y. Itoi, S. Nishiyama, S. Tsuruya, M. Masai, J. Mol. Catal. A 110 (1996) L5.
[10] D.-H. He, N. Wakasa, T. Fuchikami, Tetrahedron Lett. 36 (1995) 1059.
[11] J. Goetz, M.A. Volpe, C.E. Gigola, R. Touroude, J. Catal. 199 (2001) 338.
[12] K. Yoshikawa, Y. Iwasawa, J. Mol. Catal. A 100 (1995) 115.
[13] W. Zhou, J.M. Thomas, D.S. Shephard, B.F.G. Johnson, D. Ozkaya, T. Maschmeyer, R.G. Bell, Q. Ge, Science 280 (1998) 705.
[14] R. Raja, T. Khimyak, J.M. Thomas, S. Hermans, B.F.G. Johnson, Angew. Chem.-Int. Ed. 40 (2001) 4638.
[15] R. Raja, G. Sankar, S. Hermans, D.S. Shephard, S. Bromley, J.M. Thomas, B.F.G. Thomas, Chem. Commun. (1999) 1571.
[16] P.A. Midgley, M. Weyland, J.M. Thomas, B.F.G. Thomas, Chem. Commun. (2001) 907.
[17] S.T. Bromley, G. Sankar, C.R.A. Catlow, T. Maschmeyer, B.F.G. Johnson, J.M. Thomas, Chem. Phys. Lett. 340 (2001) 524.
[18] J.M. Thomas, B.F.G. Johnson, R. Raja, G. Sankar, P.A. Midgley, Acc. Chem. Res. 36 (2003) 20, and references therein.
[19] R. Raja, T. Khimyak, J.M. Thomas, S. Hermans, B.F.G. Johnson, Angew. Chem.-Int. Ed. 40 (2001) 4638.
[20] B. Coq, F. Figueras, Coord. Chem. Rev. 178–180 (1998) 1753–1783.
[21] M.S. Nashner, A.I. Frenkel, D.L. Adler, J.R. Shapley, R.G. Nuzzo, J. Am. Chem. Soc. 119 (1997) 7760.
[22] B.C. Gates, Chem. Rev. 95 (1995) 511.
[23] R. Raja, G. Sankar, S. Hermans, D.S. Shephard, S. Bromley, J.M. Thomas, B.F.G. Thomas, Chem. Commun. (1999) 1571.
[24] K. Tomishige, K. Asakura, Y. Iwasawa, J. Catal. 149 (1994) 70.
[25] A. Christensen, A.V. Ruban, P. Stoltze, K.W. Jacobsen, H.L. Skriver, J.K. Norskov, F. Besenbacher, Phys. Rev. B 56 (1997) 5822.
[26] P. Waszczuk, J. Solla-Gullon, H.S. Kim, Y.Y. Tong, V. Montiel, A. Aldaz, A. Wieckowski, J. Catal. 203 (2001) 1.
[27] G. Neri, A. Donato, C. Milone, R. Pietropaolo, J. Schwank, Mater. Chem. Phys. 44 (1996) 145.
[28] D.R. Rolison, P.L. Hagans, K.E. Swider, J.W. Long, Langmuir 15 (1999) 774.

[29] Q. Wei, M. Nieuwenhuyzen, F.C. Meunier, C. Hardacre, S.L. James, Dalton Trans. (2004) 1807.
[30] G. Ertl, H. Knözinger, J. Weitkamp, Preparation of Solid Catalysts, Wiley–VCH, New York, 1999.
[31] C. Moreno-Castilla, M.A. Salas-Peregrin, F.J. Lopez-Garzon, J. Mol. Catal. A 95 (1995) 223.
[32] Z.-Z. Lin, T. Okuhara, M. Misono, J. Phys. Chem. 92 (1988) 723.
[33] S. Gao, L.D. Scmidt, J. Catal. 115 (1989) 356.
[34] S. Alerasool, D. Boecker, B. Rejai, R.D. Gonzalez, Langmuir 4 (1988) 1083.
[35] G.C. Bond, B. Coq, R. Dutartre, J.G. Ruiz, A.D. Hooper, M.G. Proietti, M.C.S. Sierra, J.C. Slaa, J. Catal. 161 (1996) 480.
[36] G.C. Bond, J.C. Slaa, J. Mol. Catal. A 96 (1995) 163.
[37] A. Guerrero-Ruiz, P. Badenes, I. Rodríguez-Ramos, Appl. Catal. A 173 (1998) 313.
[38] H.M. Villulas, F.I. Mattos-Costa, L.O.S. Bulhões, J. Phys. Chem. B 108 (2004) 12898.
[39] I.M. Kodintsevt, S. Trasatti, M. Rubelt, A. Wieckowski, N. Kaufher, Langmuir 8 (1992) 283.
[40] R. Liu, H. Iddir, Q. Fan, G. Hou, A. Bo, K.L. Ley, E.S. Smotkin, Y.E. Sung, H. Kim, S. Thomas, A. Wieckowski, J. Phys. Chem. B 104 (2000) 3518.
[41] A.V. Ruban, H.L. Skriver, J.K. Norskov, Phys. Rev. B 59 (1999) 15990.
[42] C. Lee, L.D. Schmidt, J. Catal. 101 (1986) 123.
[43] T. Wang, C. Lee, L.D. Schmidt, Surf. Sci. 163 (1985) 181.
[44] G. Lauth, E. Schwarz, K. Christmann, J. Chem. Phys. 91 (1989) 3729.